

# Biomass Burning Plume due to Large Forest Fires over Siberia

Sonoyo Mukai<sup>1</sup>, Itaru Sano<sup>2</sup> and Makiko Nakata<sup>2</sup>

<sup>1</sup>The Kyoto College of Graduate Studies for Informatics

<sup>2</sup>Kindai University

## Abstract

It is well known that the biomass burning aerosols, generated by the large-scale forest fires and/or burn agriculture, have influenced the severity of air pollution. The biomass burning plumes were first analyzed based on the global distribution of hot spots by the Rapid Fire Response System provided by the measurements from the Moderate Resolution Imaging Spectrometer (MODIS), on board the satellites Terra and Aqua. In particular, the focus was on the large forest fires often occurring in early summer in Siberia. Subsequently, using the detection method of biomass burning plume from satellite measurements, an effective description of the aerosol model was generated. Finally, the aerosol characteristics of the biomass burning plume in Siberia were retrieved as an example, by applying the Method of Successive Order of Scattering (MSOS) as radiation simulation in the semi-infinite atmosphere to the data by Aqua/MODIS for May 10, 2016.

**Keywords:** Aerosol retrieval, MSOS, GLI, ADEOS-2, MODIS, Aqua

## 1. Introduction

The JAXA/GCOM-C (the Japan Aerospace Exploration Agency/Global Change Observation Mission-1) satellite will be onboard the SGLI (second generation GLI (global imager)), to be launched in December 2017. The SGLI has multiple channels, including near-UV (ultraviolet) channels of 0.38 and 0.412  $\mu\text{m}$ , and two polarization channels at red and near-infrared wavelengths of 0.67 and 0.87  $\mu\text{m}$ . It is worth noting that the near-UV measurements are helpful for the detection of carbonaceous particles, which are the main component of aerosols from biomass burning. It is known that the biomass burning plumes, generated by the large-scale forest fires and/or burn agriculture, have influenced the severity of air pollution [1]. Forest fires increase due to global warming and climate change and vice versa. This negative cycle decreases the quality of global environment and human health. The 5th IPCC

report on global warming (<https://www.ipcc.ch/report/ar5/wg1/>) [https://www.google.co.jp/?gws\\_rd=ssl](https://www.google.co.jp/?gws_rd=ssl) emphasizes the importance of studying aerosol characteristics and their temporal and spatial variations, as well as mentions the warming effect of black carbon aerosols as opposed to the cooling effect of other kinds of aerosols. However, the aerosol properties of hazardous air pollutants are still insufficiently understood. Aerosol distribution varies seasonally due to factors such as emissions, photochemical reactions and wind direction [2] [3].

In this study, we have focused on remote sensing for determining the extreme concentrations of atmospheric aerosols, namely heavy aerosol pollution. This phenomenon is called a heavy aerosol episode, or simply an “episode”, since it is an unusual phenomenon. Aerosol episodes certainly deteriorate the air quality, environment and the ecosystem. It is natural to take into account not only the biomass burning plumes, but

also other aerosol episodes, because the characteristics and distribution of atmospheric aerosols are known to be complicated. The atmospheric particles originate from both, natural factors and human activities. Of the particles that are limited to naturally originating aerosols, the first one is desert dust, often called dust storms. They are the most dynamic natural phenomena which emit a large amount of mineral dust into the atmosphere, which is then widely transported, causing serious atmospheric turbidity [4]. As far as Asia is concerned, it is well known that yellow dust causes widespread and severe air pollution there [2]. It is highly likely that large-scale aerosol episodes owing to a mixture of both natural factors and human activities have occurred. These issues would possibly be considered in future studies, while the present study deals with the severe biomass burning plumes, as agricultural biomass burning episodes continue to survive in Southeast Asia, while the big forest fire in Siberia has influenced the air quality in Asia [5].

## 2. Biomass Burning Plumes By Satellites

MODIS sensor boarded on both satellites Terra and Aqua provides the hot spots based on the Rapid Fire Response System (MYD14 Collection 5) [6] [7]. The distribution of hot spots strongly suggests the position and degree of the biomass burning plumes. It is well known that biomass burning plume is a seasonal phenomenon peculiar to a particular region. Hence, the mass concentrations of aerosols are frequently governed with spatial and/or temporal variations of biomass burning episodes. In general, the values of AOT (aerosol optical thickness) vary with time and place. However, the aerosol concentrations in Siberia in May 2003 can be said to have been strongly influenced by the forest fires there. Major forest fires have occurred there from late spring to early summer [8]. Our previous work has shown a heavy haze atmosphere, which must have originated from the big forest fire around the lake Baikal, May 20, 2003 over Siberia using the measurements by ADEOS-2/GLI

and POLDER [8].

In general, retrievals of aerosols over land, based on satellite data, are made by using three-channel or two-channel algorithms in the visible to near-infrared wavelengths [9]. However, it is difficult to distinguish between absorbing (e.g., biomass burning) and non-absorbing (e.g., sulfate) particles. Thus, the usual retrieval algorithms adopt only sulfate-type non-absorbing particles, such as standard aerosols. This limitation could be overcome by using near-UV and violet data [10] [11]. The method of using shorter wavelength data has been introduced in order to detect absorbing aerosols, such as plumes from biomass burning [12] [13] [14]. An algorithm based on the combined use of near-UV and violet data is briefly described here, as it has already been shown in our previous work based on ADEOS (Advanced Earth Observing Satellite)-2 /GLI measurements [8]. Simply put, it is a method for detecting absorbing particles, based on the ratio of reflectance at 0.40 (Band 2) and 0.38  $\mu\text{m}$  (Band 1), called AAI (Absorbing Aerosol Index) hereafter. Fig. 1 shows the numerical values of AAI cited from our previous work. The solid curve in Fig. 1 shows the histogram of AAI from the GLI data within the region denoted by the white square denoted in Fig. 2. It indicates that the mean and standard deviation values of AAI are 0.907 and 0.095, respectively. The dashed curve represents the same type of data as the solid curve, but for the minimum values of AAI during May 2003, which would be the values on ordinary days. The mean and standard deviation values of 0.870 and 0.019, respectively, can therefore be considered the standard values for ordinary, clear days. Accordingly, AAI is an indicator for absorbing particles, such as biomass burning aerosols. From Fig. 1, it can be seen that the AAI for biomass burning aerosols takes a value higher than 0.9, which means,  $\text{AAI} \approx 0.9$  must be the threshold of a biomass burning plume. It can be seen from Fig. 2 that the values of AAI are high almost all over northeast Asia.

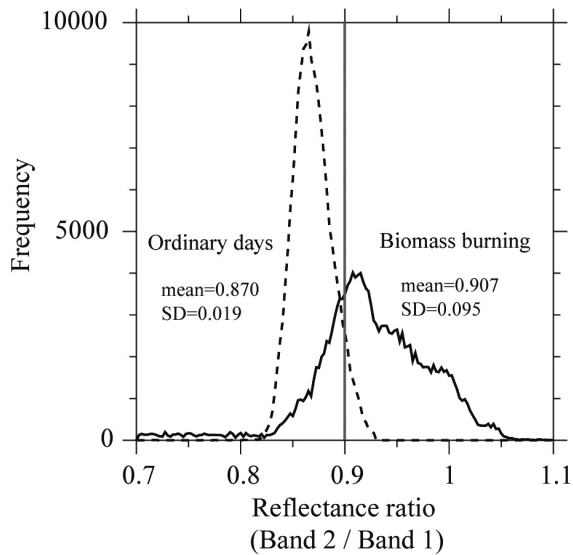


Fig. 1 The histogram of AAI, i.e. the ratio of reflectance at  $0.40 \mu\text{m}$  (Band 2) and  $0.38 \mu\text{m}$  (Band 1), over northeast Asia, derived from ADEOS-2/GLI data. The solid and dashed curves represent the histogram of the image shown in Fig. 2a on May 20, 2003 and the ordinary days during May 2003, respectively. The figure is partly cited from our previous work [8].

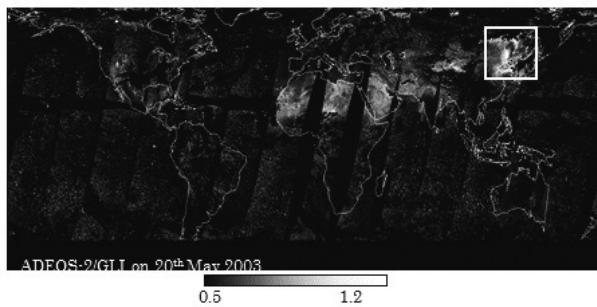


Fig. 2 Global distribution of AAI from ADEOS-2/GLI on 20 May, 2003.

### 3. AEROSOL Retrieval

#### 3-1 Aerosol model

Aerosol properties are represented by several parameters. The most basic parameter is spectral aerosol optical thickness  $AOT(\lambda)$  at a wavelength  $\lambda$ . Several other aerosol parameters, such as size distribution and refractive index, are also derived from  $AOT(\lambda)$ . According to the automatic classification of accumulated NASA/AERONET data, atmospheric aerosols have been classified into six categories [15] [16] as follows:

1. BB (biomass burning) is an aged smoke aerosol consisting primarily of soot and organic carbon;
2. RU (rural) is referred to as a clean continental

aero sol;

3. CP (continental pollution) represents anthropogenic aerosols, including various species of sulfate ( $\text{SO}_4^{2-}$ ), nitrate ( $\text{NO}_3^-$ ), OC, ammonium ( $\text{NH}_4^+$ ) and soot;
4. DP (dirty pollution) consists of the same aerosol types as CP, but at significantly higher levels;
5. DD (desert dust) is assumed to be mostly mineral soil; and
6. PM (polluted marine) consists primarily of sea salt with traces of CP.

Firstly, we focus on the size of aerosol particles. The size distributions of these six aerosol types, based on the AERONET measurements, have two modes for small ( $f$ ) and large ( $c$ ) particles in a bimodal log-normal distribution for the particle volume. Considering the aerosols here are continental, the maritime aerosol type (PM) is discarded in the present discussions. Therefore, five aerosol types {BB, RU, CP, DP, DD} are taken into account (refer to Table 1). The parameters  $V_f$ ,  $r_f$  and  $\sigma_f$  are the volume concentration, mode radius and standard deviation of small mode particles, respectively. The corresponding parameters for large mode particles are  $V_c$ ,  $r_c$  and  $\sigma_c$ . It is clear that while the six parameters are necessary for the definition of aerosol size, they are excessive for retrieving the optimized size of aerosols on a global scale. Therefore, effective simplification is required for the retrieval of size distribution of global aerosols. An assemblage of five aerosol types {BB, RU, CP, DP, DD} is treated with the k-means method by using four characteristic parameters  $\{r_f, \sigma_f, r_c, \sigma_c\}$ . These five aerosol types are iteratively assembled into k sub-clusters [17]. As a result, the optimum number of final categories is two (i.e.,  $k=2$ ), with the two sub-clusters that were obtained being {BB, RU, CP, DP} and {DD} (refer to Table 1). This statistical result is reasonable for understanding the optical and physical properties of aerosols. The former and the latter clusters represent the small anthropogenic aerosols (AA) and mineral dusts, respectively. This result is obvious in some ways before the cluster analysis,

because a cursory glance at Table 1 reveals that the four characteristic parameters  $\{r_f, \sigma_f, r_c, \sigma_c\}$ , except for volume concentration  $\{V_f, V_c\}$ , are similar to each other for {BB, RU, CP, DP} types. Therefore, we can employ the fixed values of  $\{0.144, 1.533, 3.607, 2.104\}$  for  $\{r_f, \sigma_f, r_c, \sigma_c\}$  for the AA type aerosols. Similarly, we can focus on the volume concentrations  $\{V_f, V_c\}$  alone. Here, a unique parameter ( $f$ ) of the fine particle fraction, defined as  $f = V_f / (V_f + V_c)$ , is introduced. Accordingly, the size distribution function can be approximately expressed for continental anthropogenic aerosols in the following simple form, with the unique variable of fine particle fraction ( $f$ ):

$$\frac{dV}{d \ln r} = \frac{f}{\sqrt{2\pi} \ln 1.533} \exp\left[-\frac{(\ln r - \ln 0.144)^2}{2 \ln^2 1.533}\right] + \frac{(1-f)}{\sqrt{2\pi} \ln 2.104} \exp\left[-\frac{(\ln r - \ln 3.607)^2}{2 \ln^2 2.104}\right] \quad (1)$$

Table 1 Sub-clustering of the continental aerosol types with respect to size distribution parameters partly cited from AERONET clustering works [15] [16].

	DD	BB	RU	CP	DP	
$r_f$	0.117	0.144	0.133	0.140	0.140	0.144
$\sigma_f$	1.482	1.562	1.502	1.540	1.540	1.533
$V_f$	0.077	0.040	0.013	0.032	0.032	
$r_c$	2.834	3.733	3.590	3.556	3.556	3.607
$\sigma_c$	1.908	2.144	2.104	2.134	2.134	2.104
$V_c$	0.268	0.081	0.020	0.034	0.034	

Another parameter of aerosol characteristics is refractive index. It is reasonable to consider that a mixture of various aerosol types exists in nature. A simple internal homogeneous mixing of two components is adopted using the Maxwell Garnett mixing (MGM) rule. The MGM rule provides a complex refractive index calculated using the

following equation [18] [19].

$$\varepsilon = \varepsilon_m \frac{(\varepsilon_j + 2\varepsilon_m) + 2g(\varepsilon_j - \varepsilon_m)}{(\varepsilon_j + 2\varepsilon_m) - g(\varepsilon_j - \varepsilon_m)} \quad (2)$$

where  $\varepsilon$  denotes electricity, the subscripts  $m$  and  $j$  represent the matrix and inclusion, respectively and  $g$  is the volume fraction of the inclusions, which must be less than or equal to 0.4. With regard to the accumulated AERONET measurements [15] [16], the values of the complex refractive index of AA type aerosols seems to be weakly dependent on the wavelength, at least for the visible wavelength bands. It should be noted here that the spectral absorption (i.e., the imaginary part of the refractive index) should be taken into account at NUV wavelengths [20]. We set the approximate values of  $1.404-0.004i$  and  $1.520-0.035i$  for the matrix and inclusions, respectively, for applications in the visible band data. In this approximation, the matrix and the inclusions were assumed to be weak absorbing particles such as CP-type and strong absorbers such as soot, respectively [21] [22].

The sub-clustering work of the AERONET products suggests that two kinds of aerosol properties, refractive index and size, are respectively induced from the mixing of aerosol types with the volume fraction of the inclusions ( $g$ ) and an approximate bimodal log-normal distribution, defined by the fine particle fraction ( $f$ ). In short, aerosol models are simply represented by two parameters, of  $f$  in Eq.(1) and  $g$  in Eq.(2), for the size and component of AA type particles, such as biomass burning aerosols, respectively.

### 3-2 Example of Biomass Burning Aerosol Retrieval

Figure 3 shows the distribution of hot spots superimposed on the Aqua/MODIS true color composite (RGB: Band1-4-3) images over the northeastern Siberia from 7 to 10 in May, 2016. The hot spot distribution in Fig. 3 clearly suggests the emission of a large amount of biomass burning aerosols and gaseous particles due to the big forest

fire. The hazy smoke flowing out of the region of fire origin, through the wind, can thus be recognized. The aerosol retrieval for severe biomass burning plume is then treated with these Aqua/MODIS data. For an example, dense aerosol concentrations were assumed for around central part of Fig.3d because of large AOT.

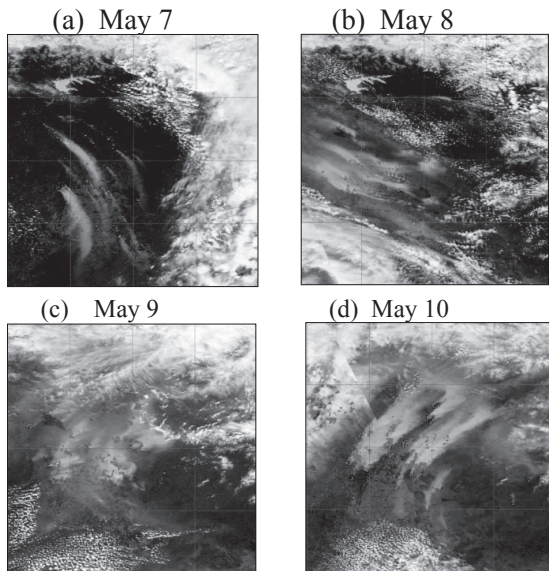


Fig.3 Distribution of hot spots superimposed on the Aqua/MODIS true color composite images over Siberia from May 7 to 10, 2016.

As mentioned above, the biomass burning aerosols are described by the two parameters of  $f$  and  $g$  alone. Therefore it is possible to derive these two parameters in a two-channel diagram with wavelengths of 0.46 and 0.55  $\mu\text{m}$ . In radiation simulations in the Earth's atmosphere, the atmosphere is assumed to be a semi-infinite, optically thick system, consisting of AA-type aerosols. In the case of the semi-infinite atmosphere, the method of successive order of scattering (MSOS) is used [1], which means, in radiation simulations by MSOS, two parameters,  $f$  and  $g$ , are desired. In other words, the size distribution takes the form of Eq. (1) with a unique parameter  $f$ , while the complex refractive index is calculated using the Maxwell Garnett internal mixing rule, represented by Eq. (2), where  $g$  represents the volume fraction of the inclusions into the matrix. The parameter  $f$  represents the fine particle fraction of the approximate bimodal log-normal size distribution

function. Thus, the two parameters,  $\{f$  and  $g\}$ , of aerosol properties for  $\{\text{size distribution and refractive index}\}$  are sufficient to carry out radiation simulations for the retrieval of AA type aerosols, based on the MSOS. Note that the basic formulation of MSOS has been shown in the previous work of this Journal [23].

The dots in Fig. 4 denote the MODIS data in the target point in Fig. 3d on May 10, 2016. The desired aerosol properties are derived from the two-dimensional interpolation of the  $(f, g)$  coordinates, whose step sizes are 0.1 and 0.01, respectively, in order to fit the MODIS data denoted by the dots. For the sake of clarity, the enlarged graph of the square surrounded by the dashed line in the original image is superimposed on the top portion of Fig. 4. From this enlarged figure, the optimized aerosol parameters were derived as  $(f^*, g^*) = (0.5, 0.31)$ . The value of  $f = 0.5$  suggests the dominance of fine particles, while  $g = 0.31$  corresponds to the absorbing carbonaceous aerosols [24]. In addition to mention, the value of AAI takes larger or equal 0.9 from a rough estimation from Aura/OMI measurements around the present target point.

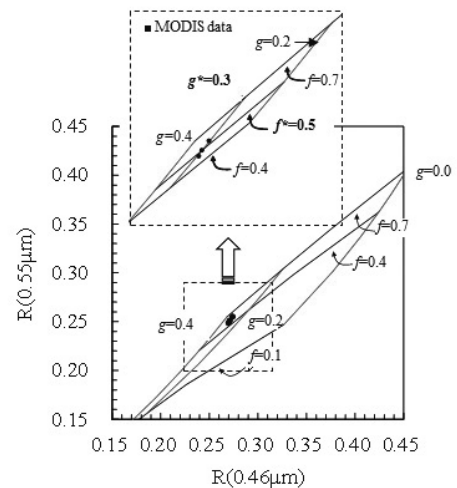


Fig. 4 The simulated values of the reflected intensity for the proposed aerosol models, described by two parameters  $(f, g)$  in a two-channel diagram of 0.46  $\mu\text{m}$  and 0.55  $\mu\text{m}$ , where the solid curves denote the results for various values of parameters  $g$  and  $f$ , respectively. The dots denote MODIS data on June 10, 2016 at the target points (around central part in Fig. 3d). The superimposed upper figure is the enlarged graph of the square surrounded by the dashed line in the bottom image.

## 4. Summary

The results of this study demonstrate that the aerosol model can be simplified for aerosol retrieval from Aqua/MODIS data in northeast Siberia. This indicates that the usage of GCOM-C / SGLI will allow a variety of issues, such as the atmospheric model itself, the surface reflectance of earth and the mixing of clouds, to be tractable because GCOM-C / SGLI will have 19 channels, including two polarization channels. It has been pointed out that the near-UV channel satellite data are effective for the retrieval of biomass burning aerosols because the carbonaceous aerosol properties are sensitive at the near-UV wavelengths [20]. We handled this issue by using 0.38 and 0.40  $\mu\text{m}$  data by ADEOS-2/GLI [8], which is consistent with the present results. It is worth mentioning that our present results are not inconsistent with the previous ones, while the computing procedure is much more effective than the previous one, as a result of the simplification of aerosol descriptions. Consequently, synthetic analysis based on the combination of visible data by MODIS, near-UV data by GLI and polarization measurements by POLDER may become practical, with the proposed procedure and results being available for a feasibility study of GCOM-C/SGLI. Furthermore, this work suggests that, with the usage of GCOM-C / SGLI, a variety of issues such as the atmospheric model itself, the surface reflectance of earth and the mixing of clouds, will be tractable by using the simplified aerosol models proposed in this work.

### Acknowledgements

The authors thank NASA for distributing the MODIS data and JAXA for ADEOS-2 data. This work was supported in part by the Global Change Observation Mission - Climate project by JAXA (no. JX - PSPC - 434796). This study was supported in part by the Global Environment Research Fund of the Ministry of Environment, Japan (S-12), and JSPS KAKENHI Grant Number 15K00528.

### References

- [1] S. Mukai, M. Yasumoto and M. Nakata, "Estimation of biomass burning influence on air pollution around Beijing from an aerosol retrieval model," *The Scientific World Journal*, Article ID 649648, doi:10.1155/2014/649648, 2014.
- [2] T. Littmann, "Dust storm frequency in Asia: Climatic control and variability," *Int. J. Climatology*, vol. 11, pp. 393–412, doi:10.1002/joc.3370110405, 1991.
- [3] S. Kinne, U. Lohmann, J. Feichter, M. Schulz, C. Timmreck, S. Ghan, R. Easter, M. Chin, P. Ginoux, T. Takemura, I. Tegen, D. Koch, M. Herzog, J. Penner, J. Pitari, B. N. Holben, R. F. Eck, A. Smirnov, O. Dubovik, I. Slutsker, D. Tanre, O. Torres, M. Mishchenko, I. Geogdzhayev, A. Chu, and Y. Kaufman, "Monthly averages of aerosol properties: A global comparison among models, satellite data and AERONET ground data," *J. Geophys. Res.*, vol. 108, D20, 4634, doi:10.1029/2001JD001253, 2003.
- [4] I. N. Sokolik, D. M. Winker, G. Bergametti, D. A. Gillette, G. Carmichael, Y. J. Kaufman, L. Gomes, L. Schuetz, and J. E. Penner, "Introduction to special section: Outstanding problems in quantifying the radiative impacts of mineral dust," *J. Geophys. Res.*, vol. 106, D16, pp. 18015-18027, doi:10.1029/2000JD 900498, 2001.
- [5] K. H. Lee, and Y. J. Kim, "Satellite remote sensing of Asian aerosols: a case study of clean, polluted and dust storm days," *Atmos. Meas. Tech.*, vol. 3, 1771-1784, doi:10.5194/amt-3-1771-2010, 2010.
- [6] C. O. Justice, L. Giglio, S. Korontzi, J. Owens, J. T. Morisette, D. Roy, J. Descloitres, S. Allesume, F. Petitcolin and Y. J. Kaufman, "The MODIS fire products," *Remote Sens. Environ.*, vol. 83, pp. 244-262. doi:10.1016/S0034-4257(02)00076-7, 2002.
- [7] L. Giglio, J. Descloitres, C. O. Justice and Y. J. Kaufman, "An enhanced contextual fire detection algorithm for MODIS," *Remote Sens. Environ.*, vol. 87, pp. 273-282. doi:10.1016/S0034-4257(03)00184-6, 2003.
- [8] I. Sano, Y. Okada, M. Mukai and S. Mukai, "Retrieval algorithm based on combined use of POLDER and GLI data for biomass aerosols," *J. RSSJ*, vol. 29, no. 1, pp. 54-59, doi:10.11440/rssj.29.54, 2009.
- [9] L. A. Remer, Y. J. Kaufman, D. Tanré, S. Mattoo, D. A. Chu, J. V. Martins, R. -R. Li, C. Ichoku, R. C. Levy, R. G. Kleidman, T. F. Eck, E. Vermote, and B. N. Holben, "The MODIS aerosol algorithm, products, and validation," *J. Atmos. Sci.*, vol. 62, pp. 947-973, doi:10.1175/JAS3385.1, 2005.
- [10] R. Höller, A. Higurashi, and T. Nakajima, "The GLI 380-nm channel – application for satellite remote sensing of tropospheric aerosol," in *Proc. EUMETSAT Meteorological Satellite Conference*, 2004.

- [11] D. Cyranoski and I. Fuyuno, "Climatologists seek clear view of Asia's smog," *Nature*, vol. 434, no. 128, doi:10.1038/434128a, 2005.
- [12] N. C. Hsu, J.R. Herman, P. K. Bhartia, C. J. Seftor, O. Torres, A. M. Thompson, J. F. Gleason, T. F. Eck and B. N. Holben, "Detection of biomass burning smoke from TOMS instruments," *Geophys. Res. Lett.*, vol. 23, pp. 745-748, doi:10.1029/96GL00455, 1996.
- [13] J. R. Herman, P. K. Bhartia, O. Torres, N. C. Hsu, C. J. Seftor and E. Celarier, "Global distribution of UV-absorbing aerosols from Nimbus-7 TOMS data," *J. Geophys. Res.*, vol. 102, pp. 16911-16922, doi:10.1029/96JD03680, 1997.
- [14] O. Torres, P. K. Bhartia, J. R. Herman, Z. Ahmad and J. Gleason, "Derivation of aerosol properties from satellite measurements of backscattered ultraviolet radiation: Theoretical basis," *J. Geophys. Res.*, vol. 103, pp. 17099-17110, doi:10.1029/98JD00900, 1998.
- [15] O. Dubovik, B. N. Holben, T. F. Eck, A. Smirnov, Y. J. Kaufman, M. D. King, D. Tanré and I. Slutsker, "Variability of absorption and optical properties of key aerosol types observed in worldwide locations," *J. Atmos. Sci.*, vol. 59, pp. 590-608, doi:10.1175/1520-0469(2002)059<0590:VOAAOP>2.0.CO;2, 2002.
- [16] A. H. Omar, J. -G. Won, D. M. Winker, S. -C. Yoon, O. Dubovik and M. P. McCormick, "Development of global aerosol models using cluster analysis of Aerosol Robotic Network (AERONET) measurements," *J. Geophys. Res.*, vol. 110, doi:10.1029/2004JD004874, 2005.
- [17] S. Mukai, I. Sano and M. Nakata, "Improvement of retrieval algorithms for heavy air pollutions," in *Proc SPIE 2016*, (in press).
- [18] P. Chýlek, and V. Srivastava, "Dielectric constant of a composite inhomogeneous medium," *Phys. Rev. B*, vol. 27, pp. 5098- 5106, doi:10.1103/PhysRevB.27.5098, 1977.
- [19] C. F. Bohren and N. C. Wickramasinghe, "On the computation of optical properties of heterogeneous grains," *Astrophysics and Space Science*, vol. 50, pp. 461-472, doi:10.1007/BF00641750, 1983.
- [20] J. M. Flores, D. F. Zhao, L. Segev, P. Schlag, A. Kiendler-Scharr, H. Fuchs, A. K. Watne, N. Blivshstein, T. F. Mentel, M. Hallquist, and Y. Rudich, "Evolution of the complex refractive index in the UV spectral region in ageing secondary organic aerosol," *Atmos. Chem. Phys.*, vol. 14, pp. 5793-5806, doi:10.5194/acp-14-5793-2014, 2014.
- [21] K. A. Fuller, W.C. Malm, and S.M. Kreidenweis, "Effects of mixing on extinction by carbonaceous particles," *J. Geophys Res.*, vol. 104, D13, pp. 15941-15954, doi:10.1029/1998JD100069, 1999.
- [22] A. M. Syer, N. C. Hsu, T. F. Eck, A. Smirnov and B. N. Holben, "AERONET-based models of smoke-dominated aerosol near source regions and transported over ocean, and implications for satellite retrievals of aerosol optical depth," *Atmos. Chem. Phys.*, vol. 14, pp. 11493-11523, doi:10.5194/acp-14-11493-2014, 2014.
- [23] S. Mukai, I. Sano and M. Nakata, An outline of the method of successive order of scattering (MSOS), *NAIS journal*, vol.11, 45-50, 2017.
- [24] S. Mukai, M. Nakata, M. Yasumoto, I. Sano and A. Kokhanovsky, "A study of aerosol pollution episode due to agriculture biomass burning in the east-central China using satellite data," *Front. Environ. Sci.*, 3:57, doi:10.3389/fenvs.2015.00057, 20

◆著者紹介

**向井 苑生** Sonoyo Mukai

京都情報大学院大学応用情報技術研究科  
環境リモートセンシングセンター (KCGI-REESIT) 教授

**佐野 到** Itaru Sano

近畿大学理工学部情報学科  
同大学院総合理工学研究科教授

**中田 真木子** Makiko Nakata

近畿大学総合社会学部准教授